QUANTUM SELF-ASSEMBLY AND PHOTOINDUCED ELECTRON TUNNELING IN PHOTOSYNTHETIC SYSTEM OF MINIMAL LIVING CELL

Arvydas Tamulis and Vykintas Tamulis

Vilnius University Institute of Theoretical Physics and Astronomy, A. Gostauto 12, LT-01108 Vilnius, Lithuania
E-mail: tamulis@itpa.lt

(Received :August 17, 2006 Accepted: March 13, 2007)

Abstract

We used quantum mechanical (QM) electron correlation interactions density functional theory (DFT) methods (*i.e.* high precision quantum mechanical calculations) to investigate self-assembled photoactive bioorganic system of artificial minimal living cell. The cell system studied is based on peptide nucleic acid (PNA) and consists of 333 atoms (not including the associated water solvent shells) and is 3.0 nm in diameter. The electron correlations interaction originating the hydrogen bonds and Van der Waals weak chemical bonds that increase due to the addition of a polar solvent (water) molecules, fatty acid (FA), precursor fatty acid (pFA) molecules and waste pieces of the pFA molecules play a critical role in the QM interaction based self-assembly of the photosynthetic center and functioning of the photosynthetic processes of the artificial minimal living cell. The distances between the separated sensitizer, precursor fatty acid, and water molecules are comparable to Van der Waals and hydrogen bonding radii. As a result these nonlinear quantum interactions compress the overall system resulting in a smaller gap between the HOMO and LUMO electron energy levels and photoexcited electron tunneling occurs from the sensitizer a 1,4-bis(N,N-dimethylamino) naphthalene to pFA molecules. The electron tunneling and associated light absorption of most intense transition as calculated by the time dependent density functional theory (TD DFT) method differs from spectroscopic experiments by only 0.3 nm, which is within the value of experiment errors. This agreement implies that the quantum mechanically self-assembled structure of minimal cell very closely approximates the realistic one.

Keywords

quantum self-assembly of photosynthetic centers, measure of the complexity of artificial minimal living cell

1. Introduction

The main features of regular and artificial bioorganic life based on DNA, RNA and PNA are growing, multiplying and information processing. Modern quantum mechanical methods provide powerful tools for theoretical modeling and analysis of biomolecular electronic and spectra structure [1-3] and may be used to guide the synthetic effort of more effective photosynthetic systems providing the light harvesting and growth.

The artificial minimal living cells or protocells [4, 5] are based on PNA (see Figure 1). PNA is similar to DNA but has a peptide-based backbone, as opposed to DNA's sugar-phosphate backbone. PNA is able to form very stable duplex structures with the same complementary Watson-Crick pairing between the nucleobases (B).

The diameter of the experimentally made minimal living cell is only 5 nm [4, 5]. Therefore all their processes including self-assembly and absorption of light could be investigated using quantum (wave) theory.

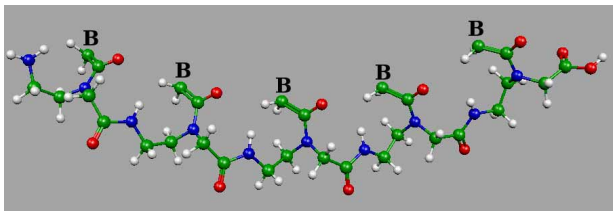

Figure 1. PNA has a peptide-based backbone. Carbon atoms and their associated covalent bonds are shown as green spheres and sticks, hydrogens are in light grey, oxygens – red, nitrogens – blue. B means attached nucleobase molecule.

The main difference from classical (Newtonian) theory is that quantum particles including the bioorganic supramolecules which self-organize into the minimal cells, behave as waves rather than discrete particles with definitive positions and momenta. For example, valence electrons of supramolecules (which mainly determine features of nano-size protocells) possess strict quantum states and discrete quantum electronic UV-VS, vibrational, NMR, EPR, etc. spectra. The entire minimal cell might be considered to be a molecular electronics device that self-assembles according to quantum correlated electron interaction potentials and that absorbs light and carries on its metabolism according to quantum electron excitation and tunneling equations.

The main purpose of this article is to find the general rules of quantum mechanical self-assembly and charge transfer in the artificial minimal living cells that are being synthesized [4, 5], and to predict the new trends of more effective synthesis of photosynthetic centers. The current work uses larger supramolecular systems and more exact quantum mechanical methods than our earlier works [1-3]. This article provides a collection of quantum

mechanical tools and their application to a variety of minimal cell photosynthetic processes, while this article also provides a perspective of the requirements for success in the synthesis of new forms of living organisms.

2. Procedure/Methodology

Our quantum simulations of single bioorganic molecules possessing closed electronic shells start from a trial geometry (Cartesian coordinates of the nuclei). Using restricted Hartree-Fock (HF) and a density functional theory (DFT) approached by the Gaussian 03 [6], GAMESS-US [7] or ORCA [8, 9] program packages, we obtain the lowest molecular energy, which depends on these coordinates parametrically. A subsequent standard geometry optimization procedure [6-11] minimizes the energy with respect to the nuclear positions. Special care is required to verify that the obtained optimal molecular structure is a global minimum in the phase space of the nuclear (3n-6, n being the number of atoms) degrees of freedom.

In order to obtain accurate results in investigating supermolecules, two factors need to be accounted for: i) the quality of the density functional and ii) the quality of the molecular orbitals (extent of the phase space of the single-electron states). For simple covalently bonded molecules we chose Becke's 3 parameter exchange functions [12] with non-local Lee-Yang-Parr electron correlations [13] (DFT B3LYP), and PBEPBE [6, 8, 9, 14], and PBELYP [7, 14] models. Currently, the B3LYP method is considered to be the most appropriate method to take into account electron correlations in large closed-shell supermolecules of which atoms are linked by covalent bonds (*i.e.*, there are no Van der Waals nor hydrogen bonds between atoms in a single molecule) [15, 16]. For simulations of the self-assembly of bioorganic supramolecules in which the separate molecules are associated by hydrogen bonds or Van der Waals forces we used PBEPBE [6, 8, 9, 14], and PBELYP [7, 14] methods. In these two methods, exchange functionals include some electron correlation effects at larger distances that provide relatively good descriptions of the Van der Waals forces and hydrogen bonds. To obtain accurate optimal molecular geometries for single molecules, we use the 6-311G** basis set which includes (5d, 7f) polarized atomic orbitals. For self-assembly of pairs of bioorganic molecules we add diffusion orbitals of the 6-31++G** basis set (the standard tables [17] give the appropriate basis set description).

The above-mentioned 6-311++G** basis set convention was adopted by John Pople and coworkers. The basis set structure is given for the whole molecule, rather than a particular atom. The notation also emphasizes the split valence (SV) nature of these sets. Symbols like n-ijG or n-ijkG are encoded as follows: n – the number of primitives for the inner shells; ij or ijk - the number of primitives for contractions in the valence shell. The ij notation describes sets of valence double zeta quality and ijk, sets of valence triple zeta quality. Generally, in the basis sets derived by Pople's group, the s and p contractions belonging to the same "electron shell" (*i.e.* corresponding formally to the same principal quantum number n) are folded into an sp-shell. In this case, the number of s-type and p-type primitives is the same, and they have identical exponents. However, the coefficients for the s- and p-type contractions are different. The symbol "*" is used to indicate when Pople's basis sets are augmented with d- or f-type polarization functions: n-ijG* or n-ijkG* when this is done only for heavy atoms; and n-ijG** or n-ijkG** when done for all atoms together with p-functions for hydrogen atoms.

The basis sets are also frequently augmented with the so-called diffuse functions. These are very shallow Gaussian basis functions, which more accurately represent the "tail" portion of the atomic orbitals, which are distant from the atomic nuclei. These gaussians have very small exponents and decay slowly with distance from the nucleus. The diffuse gaussians are usually s- and p-type, though sometimes diffuse polarization functions are also used. Diffuse functions are necessary for a correct description of anions and weak bonds (*e.g.* hydrogen bonds) and are frequently used for calculation of properties such as dipole moments, and polarizabilities, *etc.* The inclusion of diffuse functions is indicated with the "+" sign: n-ij+G or n-ijk+G when one diffuse s-type and p-type gaussian with the same exponent is added to a standard basis set for heavy atoms; and n-ij++G or n-ijk++G when one diffuse s-type and p-type Gaussian is added for heavy atoms together with one diffuse s-type gaussian for hydrogen atoms. Table 1 lists the availability of diffuse and polarization functions and the range of applicability for each built-in Gaussian03 [6] and ORCA [8, 9] program packages basis set we use.

Table 1 The function availability and range of applicability for each built-in basis set in Gaussian03 [6] and ORCA [8, 9] program packages.

Basis set	*Applies to atoms*	*Polarization functions*	*Diffuse functions*
3-21G	H-Xe	* *or* **	+
6-31G	H-Kr	(3df,3pd)	++
6-311G	H-Kr	(3df,3pd)	++

The chemical formulas of the molecules used in the simulated version of minimal cell are **1)** 1,4-bis(N,N-dimethylamino)naphthalene – $(CH_3)_2$-N-C_8H_6-N-$(CH_3)_2$, and **2)** cytosine – $C_4H_5N_3O$, and **3)** precursor of fatty acid – C_6H_5-CO-(CH_2)-O-CO-$(CH_2)_3$-CH_3, and **4)** head (the waste piece) of the precursor of fatty acid – C_6H_5-CO-CH_3, **5)** and fatty acid – HO-CO-$(CH_2)_3$-CH_3 (see Figure 2).

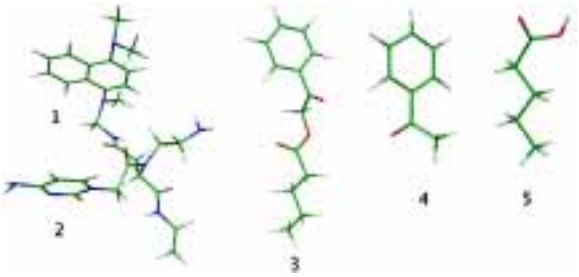

Figure 2. The molecules used in the simulated version of minimal cell are fragment of PNA supermolecule with attached **1)** 1,4-bis(N,N-dimethylamino)naphthalene, and **2)** cytosine molecules, and **3)** precursor of fatty acid, and **4)** head (the waste piece) of the precursor of fatty acid, **5)** and fatty acid molecules. Carbon atoms and their associated covalent bonds are shown as green sticks, hydrogens are in light grey, oxygens – red, nitrogens – blue.

Quantum modeling of the self-assembly of nano-structures in PNA based minimal living cells was performed using the software we developed for building PNA double helices.

The geometries of the constituent molecules and their pairs were individually optimized using the PBELYP [7, 14] method with the 6-311++G** basis set implemented in the GAMESS-US program package which is installed in dual processor Opteron servers Linux cluster of our Theoretical Molecular Electronics and Spintronics research group and with the PBEPBE method [6, 14] using the 6-311++G** basis set [17] implemented via the Gaussian03 program package on the Los Alamos National Laboratory (LANL) SGI Altix 3000 supercomputer.

We used TD DFT PBEPBE method [6] with the 6-31G basis set together with COSMO water solvent method [18] in the ORCA program package which is installed on our dual processor Opteron servers Linux cluster to calculate the absorption spectra and the relative positions of the HOMO and LUMO eigenvalues of Schroedinger equation of the pFA and various separate sensitizer molecules, that is to say, 1,4-bis(N,N-dimethylamino)naphthalene, and 1,4-dihydroquinoxaline, and 7,8-dimethylisoalloxazine [2]. Analysis of the results showed that these sensitizers were good candidates for use in artificial minimal cells because their HOMO electron energy levels were energetically high enough relative to the LUMO electron energy level of the pFA molecule and their absorption spectra were in the visible region [2]. These investigations were performed without the presence of surrounding water molecules. Therefore the absorption spectra were strongly shifted to the blue region. Thus the resulting analysis was valuable only for comparison of HOMO and LUMO eigenvalues relationships, but not for obtaining the real wavelengths of the absorption spectra.

By investigating a number of different models [2, 3, 20] of the photosynthetic systems and each subsequent model including more water and fatty acid molecules, we were able to quantify this effect. The rather good model shown in the paper [19] gave an excitation photon wavelength of 440.0 nm, which was comparing enough well with the experimental value of 450.0 nm [5]. It was possible that the remaining small (450.0-440.0=10 nm) difference understood by the greater number of water and fatty acid molecules found in the real system in comparison with the previous models [2, 3]. The slightly shorter wavelength given by the model was also consistent with our finding that the inclusion of more water and fatty acid molecules in the models resulted in longer wavelengths for the absorption spectrum.

All figures were created by Molekel software [20] in this article.

3. Quantum modeling of self-assembly and photoinduced electron transfer in PNA based artificial minimal cell

3.1. Quantum modeling of self-assembly of minimal living cell.

We have investigated geometry optimization of a minimal cell section containing a cytosine bearing PNA fragment with an attached 1,4-bis(N,N-dimethylamino)naphthalene sensitizer, six fatty acid, two pFA, two the waste pieces of the pFA molecules, and 18 water molecules constituting the micellar container's inner monolayer, using the electron correlated PBEPBE method with the 3-21G basis set (see Figure 3). The cell system studied is consisted of 333 atoms (not including the associated water solvent shells) and is 3.0 nm in diameter.

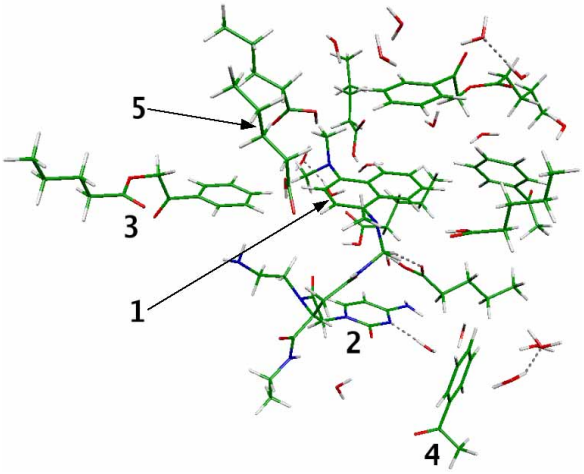

Figure 3. Image of the geometric and electronic structure of a system consisting of 333 atoms and containing fragment of PNA molecule with attached **1)** 1,4-bis(N,N-dimethylamino)naphthalene, **2)** cytosine molecules, and two, **3)** precursor of fatty acid molecules (in the left and in the top-right), and two, **4)** head the waste pieces of the precursor of fatty acid molecules (in the bottom and in the right), and six, and **5)** fatty acid molecules and water molecules that were optimized using the PBEPBE/3-21G model. Carbon atoms and their associated covalent bonds are shown as green sticks, hydrogens are in light grey, oxygens – red, nitrogens – blue. Hydrogen bonds are depicted by dashed lines.

The water molecules, which surrounded the entire bioorganic photosynthetic complex were found to stabilize the system. Thereby all the interatomic distances were reduced (all H-bonds are marked in dash lines in Figure 3). The water molecules organized into nano ice-like substructures. One of such a nano ice-like substructures is self-organized in the right-bottom in Figure 3, and another in the top-right. It is only because of the hydrogen and Van der Waals bonds among the cytosine-PNA, fatty acid, pFA, waste pieces of the pFA molecules and water molecules that this system with 3.0 nm larger diameter exists. The distances among the separated sensitizer, fatty acid, pFA, waste pieces of the pFA molecules and water molecules are comparable to Van der Waals and hydrogen bonding radii, and therefore we may regard the minimal cell as single electron conjugated supramolecule that we can deal with using an electron correlated model. Since cytosine-PNA fragment interacts with fatty acid, and pFA, and waste pieces of the pFA molecules and with water molecules through their correlated electrons, intermolecular distances and surface area calculations are critical in understanding the time dependent electron tunneling processes associated with the various excited states of this minimal cell. These nonlinear quantum interactions compress the overall system resulting in a smaller gap among the HOMO and LUMO electron energy levels.

It is important to say that only quantum mechanical electron correlation TD-DFT experiments with minimal protocells gives results to be exactly comparable with spectroscopic results and all other more simplyfied QM methods such as local gradient DFTor *ab initio* Hartree-Fock gives structures and spectra far from the experimentaly measured.

3.2. Quantum mechanical calculations of absorption spectrum of minimal living cell.

The absorption spectrum (see Table 2) of this photosynthetic system was calculated optimizing geometry by using the TD DFT PBEPBE method [8, 9] with the 6-31G basis set together with COSMO [18] water solvent method.

This latest and indeed the most realistic model shown in the present paper gave an excitation photon wavelength of 450.3 nm, which was comparing exactly with the experimental value of 450.0 nm [5]. The small (10 nm) difference obtained in the previous paper [19] was compensated for including to the previous rather good system by two waste pieces of the pFA molecules in addition to the water, fatty acid, and pFA molecules. The waste piece of the pFA molecule possesses the aromatic ring (see Figure 2) therefore conjugated electrons strongly interact with other molecules in this system generating Van der Waals forces. These additional Van der Waals interactions of the introduced two waste pieces of the pFA molecules with the water, fatty acid, and pFA molecules shortened all the inner micelle diameter and resulted in a even smallest gap between the HOMO and LUMO electron energy levels. This was also consistent with our finding that the inclusion of more molecules in the models resulted in longer wavelengths for the absorption spectrum. The shift of the absorption spectrum to the red for the artificial protocell photosynthetic center might be considered as the measure of the complexity of this system.

This our found method of designing of photosynthetic centres of minimal cells makes possible to search for new sensitizers [21].

3.3. Quantum modeling of electron tunneling in excited states of minimal living cell.

We have performed calculations using TD DFT PBEPBE method [8, 9] with the 6-31G basis set together with COSMO [18] water solvent method of the difference of electron charge density (excited-state - ground-state) for the conjugated cytosine-1,4-bis(N,N-dimethylamino)naphthalene supermolecule, six fatty acid, two pFA molecules, and two waste pieces of the pFA molecules, and visualized the electron charge tunneling associated with certain excited state transitions (see examples in the Figures 4-6).

The calculation indicated that the most intense electron charge transition from the conjugated cytosine-PNA fragment-1,4-bis(N,N-dimethylamino)naphthalene supermolecule to one of the pFA molecules was for the eighth excited state (HOMO-1→LUMO+1) transition and had an energy and wavelength of 2.753 eV and 450.3 nm respectively (see Table 2 and Figure 4).

The electron cloud hole in Figures 4, 5 and 6 is indicated by the dark blue color while the transferred electron cloud location is visualized by the grey color.

We have also found a relative intense electron charge transition for the tenth excited state mainly from the 1,4-bis(N,N-dimethylamino)naphthalene

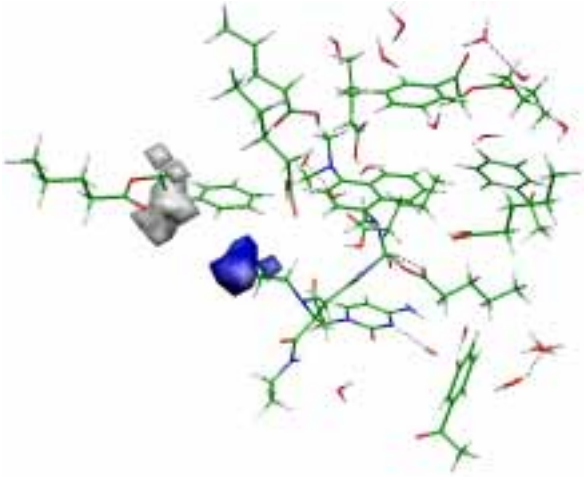

Figure 4. Visualization of the electron charge tunneling associated with the eighth excited state. The transition is from the conjugated cytosine-PNA fragment-1,4-bis(N,N-dimethylamino)naphthalene supermolecule (in the left-bottom) to the one of the pFA molecules (in the left). Carbon atoms and their associated covalent bonds are shown as green sticks, hydrogens are in light grey, oxygens – red, nitrogens – blue.

Table 2 Excitation transitions energies of a cytosine-PNA fragment covalently bonded to a 1,4-bis(N,N-dimethylamino) naphthalene sensitizer, six fatty acid, two pFA molecules, two the waste pieces of the pFA molecules and 18 water molecules, as calculated using the TD PBEPBE method with the 6-31G basis set together with water solvent COSMO method [18]. The weight of the individual excitations are given if larger than 0.01. Arrow → indicates the direction of individual electron transition from ground state HOMO-m to certain excited state LUMO+n.

Excited State #	Individual transitions HOMO-m → LUMO+n			Weight of individual transition	Energy (eV)	Wavelength (nm)	Oscillator strength (arbitrary
1	HOMO	→	LUMO	0.99	2.161	573.7	0.000016
2	HOMO	→	LUMO+1	0.99	2.362	524.8	0.000022
3	HOMO	→	LUMO+2	0.99	2.371	522.9	0.000000
4	HOMO	→	LUMO+3	0.99	2.520	491.9	0.000221
5	HOMO-1	→	LUMO	1.00	2.549	486.3	0.000000
6	HOMO-2	→	LUMO	0.99	2.571	482.2	0.000006
7	HOMO	→	LUMO+4	0.99	2.711	457.4	0.000080
8	HOMO-1	→	LUMO+1	0.99	2.753	450.3	0.000902
9	HOMO-1	→	LUMO+2	0.99	2.759	449.3	0.000000
10	HOMO-2	→	LUMO+1	0.99	2.773	447.1	0.000409
11	HOMO-2	→	LUMO+2	1.00	2.781	445.8	0.000000
12	HOMO-1	→	LUMO+3	0.99	2.908	426.3	0.000002
13	HOMO-2	→	LUMO+3	0.99	2.930	423.1	0.000061
14	HOMO	→	LUMO+5	0.01	3.004	412.7	0.000732
15	HOMO-3	→	LUMO	0.99	3.009	412.1	0.000065

molecule to the same pFA molecule (HOMO-2→LUMO+1) equal to 447.1 nm (2.773 eV) (see Table 2 and Figure 5).

We have also found a relative intense electron charge transition for the fourteenth excited state (412.7 nm or 3.004 eV) from the 1,4-bis(N,N-dimethylamino)naphthalene molecule to the second of pFA molecules (weight of individual transition HOMO→LUMO+6 is equal to 0.99) (see Table 2 and Figure 6).

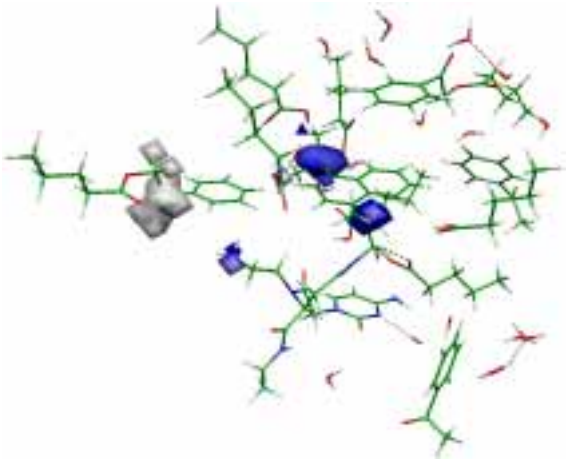

Figure 5. Visualization of the electron charge tunneling associated with the tenth excited state. The transition is mainly from the sensitizer 1,4-bis(N,N-dimethylamino)naphthalene molecule to the one of pFA molecules (in the left).

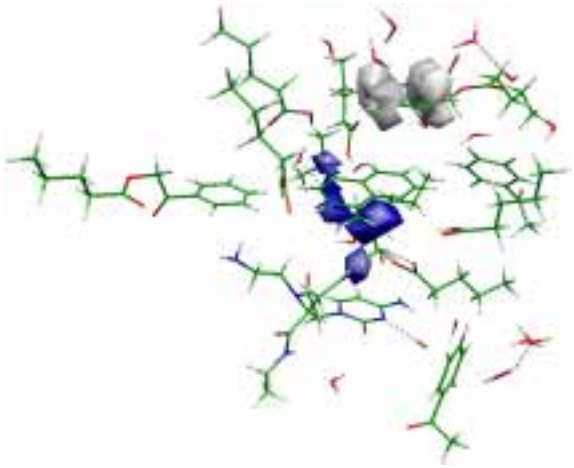

Figure 6. Visualization of the electron charge tunneling associated with the fourteenth excited state. The transition is from the sensitizer 1,4-bis(N,N-dimethylamino)naphthalene molecule to the second of pFA molecules (in the top-right).

The electron tunneling intense transitions of the 8^{th}, 10^{th} and 14^{th} excited states should induce metabolic photodissociation of pFA molecule because the transferred electron cloud is located on the head (the waste piece) of pFA molecule (see Figures 4, 5 and 6). The new fatty acid from dissociated pFA molecule will join to minimal cell, and therefore this minimal cell will grow and later spontaneously break in two new minimal cells and

once again will use pFA molecules during the photo excitation processes for generation the new FA molecules, etc. This photoinduced autocatalytic bioorganic system was experimentaly proved in the papers [4, 5], and called in LANL "Protocell Assembly" project as minimal artificial living cell.

Our last two quantum self-assembled models of the photosynthetic systems includes a PNA fragment which is covalently bonded to a $Ru(bipyridine)_3^{2+}$ [21] or bis(4-dimethylamino-2-dihydroxyphenyl)squarine sensitizer, and pFA and water molecules. It was confirmed by the small differences (0.2 nm) of the experimental absorption spectra peaks [5] in comparison with our QM calculated that our chosen method of designing single electron nano photocells might be useful not only for artificial organisms but also for wide implementation in the nano photodevices and molecular computers [22].

Conclusions

An important finding of our investigation of the quantum self-assembly of photosynthetic centers and the functioning of the photosynthetic process is the critical role played by the nonlinear quantum electron correlated hydrogen bonds and Van der Waals interactions that result from the addition of water and fatty acid molecules. The distances between the separated sensitizer, fatty acid precursor (pFA) and water molecules are comparable to Van der Waals and hydrogen bonding radii, and therefore we may regard minimal cells as single electron conjugated supramolecules that we can deal with using an electron correlated TD DFT methods. These nonlinear quantum interactions compress the overall system resulting in a smaller gap among the HOMO and LUMO electron energy levels and photoexcited electron tunneling from sensitizer to pFA molecules.

Our presenting quantum self-assembled model of the photosynthetic systems includes a cytosine-PNA fragment which is covalently bonded to a 1,4-bis(N,N-dimethylamino) naphthalene sensitizer, and six fatty acid, two pFA molecules, and two heads (the waste pieces) of the pFA molecules of constituting the 3.0 nm size micellar container's inner monolayer with water. The correspondence of our calculated absorption spectra peak 450.3 nm with the experimental one indicate that we obtained realistic structure of photosynthetic center of minimal cells reported in [4, 5], and makes possible to search for new sensitizers [21].

Quantum mechanical electron correlation experiments of self-assembly of above described artificial minimal living cells show that these cells are complex systems because only entire ensembl of PNA, sensitizer, pFA, FA and water molecules is stable and performs quantum photosynthetic processes. Removing the small part of nucleobase, FA and water molecules leads to the structural changes in comparison with realistic structures and the difference from the spectroscopic values of photoexcited electron tunneling from sensitizer (1,4-bis(N,N-dimethylamino)naphthalene to pFA molecules. QM electron correlation experiments of self-assembly of artificial minimal cells removing the main part of nucleobase, FA and water molecules lead to the degradation of these cells. We can state that the inclusion of ever more water, fatty acid, pFA molecules, waste pieces of the pFA molecules and nucleobase molecules in the different artificial minimal cells results in a shift of the absorption spectrum to the red for the artificial protocell photosynthetic center, leading to an ever closer approach to the real experimental value, and indicates the measure of the complexity of this quantum complex system, *i.e.* a minimal protocell. It is important to say that only QM electron correlation TD-DFT experiments with minimal protocells give results to be exactly comparable with spectroscopic results and all other more simplyfied QM methods such as local gradient DFTor *ab initio* Hartree-Fock gives structures and spectra far from the experimentaly measured.

The correspondence of experimental absorption spectra peaks and our QM calculated confirmed that our chosen method of designing single electron nano protocells might be useful not only for artificial minimal living cells but also for wide implementation in the nano photodevices, and molecular computers [22].

Acknowledgments

The work was funded via the PACE (Programmable Artificial Cell Evolution), the European Integrated Project in the EU FP6-IST-FET Complex Systems Initiative, and partially by the Agency for International Science and Technology Development Programmes.

The authors also thank the Los Alamos National Laboratory Protocell Assembly LDRD DR project for use of the LANL SGI Altix 3000 machine and their installed Gaussian 03 program package.

References

1. Tamulis, A., Tamuliene, J. and Tamulis, V. Quantum mechanical design of photoactive molecular machines and logical devices, p.p. 495-553, in Handbook of photochemistry and photobiology, Vol. 3 Supramolecular photochemistry, Nalwa, H.S. Ed. American Scientific Publishers, 2003.
2. Tamuliene, J. and Tamulis A. Quantum mechanical investigations of self-assembled system consisting of peptide nucleic acid, sensitizer, and lipid precursor molecules, Lithuanian Journal of Physics 45, 167-174 (2005).
3. Tamulis, A., Tamulis, V. and Graja, A. Quantum mechanical modeling of self-assembly and photoinduced electron transfer in PNA based artificial living organism, Journal of Nanoscience and Nanotechnology 6, 965-973 (2006).
4. Rasmussen, S., Chen, L., Nilsson, M. and Abe, S. Bridging nonliving and living matter, Artificial Life 9, 267-316 (2003).
1. Rasmussen, S., Bailey, J., Boncella, J., Chen, L., Collins, G., Colgate, S., DeClue, M., Fellermann, H., Goranovic, G., Jiang, Y., Knutson, C., Monnard, P.-A., Moufouk, F., Nielsen, P., Sen, A., Shreve, A., Tamulis, A., Travis, B., Weronski, P., Woodruff, W., Zhang, J., Zhou, X. and Ziock, H., Assembly of a minimal protocell, in Protocells: Bridging nonliving and living matter, Rasmussen, S., Bedau, M., Chen, L., Krakauer, D., Deamer, D., Packard, N., and Stadler, P. Ed., MIT Press, 2007 (in press).

6. Frisch, M. J., Trucks, G. W., Schlegel, H. B., Scuseria, G. E., Robb, M. A., Cheeseman, J. R., Montgomery, J. A. Jr., Vreven, T., Kudir, K. N., Burant, J. C., Millam, J. M., Ivengar, S. S., Tomasi, J., Barone, V., Mennucci, B., Cossi, M., Scalmani, G., Rega, N., Petersson, G. A., Nakatsuji, H., Hada, M., Ehara, M., Toyota, K., Fukuda, R., Hasegawa, J., Ishida, M., Nakajima, T., Honda, Y., Kitac, O., Nakai, H., Klene, M., Li, X., Knox, J. E., Hratchian, H. P., Cross, J. B., Adamc, C., Jaramillo, J., Gomperts, R., Stratmann, R. E., Yazyev, O., Austin, A. J., Cammi, R., Pomelli, C., Ochterski, J. W., Ayala, P. Y., Morokuma, K., Voth, G. A., Salvador, P., Dannenberg, J. J., Zakrzewski, V. G., Dapprich, S., Daniels, A. D., Strain, M. C., Farkas, O., Malick, D. K., Rabuck, A. D., Raghavachari, K., Foresman, J. B., Ortiz, J. V., Cui, Q., Baboul, A. G., Clifford, S., Cioslowski, J., Stefanov, B. B., Liu, G., Liashenko, A., Piskorz, P., Komaromi, I., Martin, R. L., Fox, D. J., Keith, T., Al-Laham, M. A., Peng, C. Y., Nanayakkara, A., Challacombe, M., Gill, P. M. W., Johnson, B., Chen, W., Wong, M. W., Gonzalez, C. and Pople, J. A., Gaussian 03, Revision C.02, Gaussian, Inc., Wallingford CT, 2004.
7. Schmidt, M. W., Baldridge, K. K. Boatz, J. A., Elbert, S. T., Gordon, M. S., Jensen, J. H., Koseki, S., Matsunaga, N., Nguyen, K. A., Su, S., Windus, T. L., Dupuis, M. and Montgomery J. A. General atomic and molecular electronic structure system, Journal of Computational Chemistry 14, 1347-1363 (1993). http://www.msg.ameslab.gov/GAMESS/GAMESS.html
8. Neese, F. ORCA - an ab initio, density functional and semiempirical program package, Version 2.4. Max-Planck-Institut fuer Bioanorganische Chemie, Muelheim and der Ruhr, 2004
9. Neese, F. A spectroscopy oriented configuration interaction procedure, Journal of Chemical Physics 119, 9428-9443 (2003).
10. Cook, D. B. Handbook of computational quantum chemistry, Oxford University Press, New York, 1998.
11. Dreizler, R. M. and Gross E. K. U., Density functional theory, Springer-Verlag, Berlin, 1990
12. Becke, A. D. Density-functional exchange-energy approximation with correct asymptotic-behavior, Physical Review A 38, 3098-3100 (1988).
13. Lee, C. T., Yang, W. T. and Parr, R. G. Development of the Colle-Salvetti correlation-energy formula into a functional of the electron density, Physical Review B 37, 785-789 (1988).
14. Perdew, J. P., Burke, K. and Ernzerhof, M. Generalized gradient approximation made simple, Physical Review Letters 77, 3865-3868 (1996).
15. Springborg, M. Ed., Density-functional methods in chemistry and materials science, John Wiley & Sons, Chichester-Toronto, 1997.
16. Jensen, F., Introduction to Computational Chemistry. John Wiley & Sons, Chichester-Toronto, 1999.
17. Extensible Computational Chemistry Environment Basis Set Database, Environmental and Molecular Sciences Laboratory at Pacific Northwest Laboratory, P.O. Box 999, Richland, Washington 99352, USA.
18. http://www.cosmologic.de/ChemicalEngineering/theory_background.html
19. Tamulis, A., Tamulis, V., Ziock, H. and Rasmussen, S. Influence of water and fatty acid molecules on quantum photoinduced electron tunneling in photosynthetic systems of PNA based self-assembled protocells, in Multi-scale Simulation Methods for Materials, Ross, R. and Mohanty, S. Ed., John Wiley & Sons, Inc., New Jersey, 2007 (in press).
20. http://www.cscs.ch/molekel/
21. Tamulis, A., Tamulis, V., A., Ziock, H. and Rasmussen, S. Quantum processes in 8-oxo-Ru(bipyridine)$_3^{2+}$ photosynthetic systems of artificial minimal cells, Lithuanian Journal of Physics 47, No 2 (2007) (in press).
22. Tamulis, A. and Tamulis, V. Quantum mechanical self-assembling of artificial minimal cells and control by molecular electronics and spintronics logical devices, Lithuanian Journal of Physics 47, No 3 (2007) (in press).